

## Research Article

# A Genetic and Simulated Annealing Combined Algorithm for Optimization of Wideband Antenna Matching Networks

Aixin Chen,<sup>1</sup> Tiehua Jiang,<sup>1</sup> Zhizhang Chen,<sup>2</sup> and Yanjun Zhang<sup>1</sup>

<sup>1</sup>School of Electronic and Information Engineering, Beihang University, Beijing 100191, China

<sup>2</sup>Department of Electrical and Computer Engineering, Dalhousie University, Halifax, NS, Canada B3J 2X4

Correspondence should be addressed to Aixin Chen, axchen@buaa.edu.cn

Received 8 December 2011; Revised 15 February 2012; Accepted 27 February 2012

Academic Editor: Lance Griffiths

Copyright © 2012 Aixin Chen et al. This is an open access article distributed under the Creative Commons Attribution License, which permits unrestricted use, distribution, and reproduction in any medium, provided the original work is properly cited.

A genetic and simulated annealing combined algorithm is presented and applied to optimize broadband matching networks for antennas. As a result, advantages of both the genetic algorithm (GA) and simulated annealing (SA) are taken. Effectiveness and efficiency of the presented combined algorithm are demonstrated by optimization of a wideband matching network for a VHF/UHF discone-based antenna. The optimized parameters provide significant improvements of VSWR and transducer power gain for the antenna.

## 1. Introduction

Development of wideband, low-profile, and miniature antennas has garnered attention in recent years due to demands for high-speed and small devices and systems. On the other hand, wideband and miniaturization are two contradicting requirements for antenna design. One helpful way to mitigate this problem is to employ a wideband matching network.

In the past, designs of antenna impedance matching networks have been focused on multiple-input multiple-output matching [1], non-Foster matching [2], adaptive impedance matching [3], RFID dual-band matching [4], and matching with metamaterials [5].

In these designs, optimization techniques were employed to develop wideband matching networks. For instance, the real frequency method was introduced in [6, 7]. The combination of the real frequency technique and GA was developed in [8] for broadband loaded wire antennas. A real-coded GA was reported in [9] for broadband HF antenna matching network. A GA-based optimization method was presented in [10] to design “on-body” matching networks for VHF/UHF antennas. SA algorithm and the finite element method (FEM) were used to optimize ultra-wideband monopole antennas [11], and a multiobjective particle swarm optimization (PSO) was applied to LC filter tuning [12].

Among the optimization methods, GA is robust; however, as stated in part A of Section II of [9], “usually a GA

converges very fast to the neighborhood of the solution, but then it does it very slowly or can even stagnate”. Also, part E of Section II of [9] indicated “the excessive slow convergence of conventional genetic algorithms after a number of generations”; in other words, GA may converge slowly to an optimized solution when it is near the solution. On the other hand, SA has better optimization efficiency if with good initial parameters [13]. To solve this dilemma, a GA-SA-combined algorithm is introduced in this paper; it takes the advantages of both methods, resulting in a robust and fast optimization method. The GA-SA algorithm is then applied to optimize a wideband matching network for a discone-based antenna [14] over the band of 225 MHz to 400 MHz; the results demonstrated effectiveness and efficiency of the method.

This paper is organized as follows: first, the configuration of the matching network to which the presented GA-SA is applied is described in Section 2; then the combined GA-SA algorithm is described in Section 3. The optimization results of the GA-SA algorithm are presented in Section 4. Finally, the conclusions of this paper are made in Section 5.

## 2. The Wideband Matching Network

The wideband matching network under consideration in this paper as an example is shown in Figure 1. It consists of three parts: a three-resistor  $\pi$  network, two T-networks,

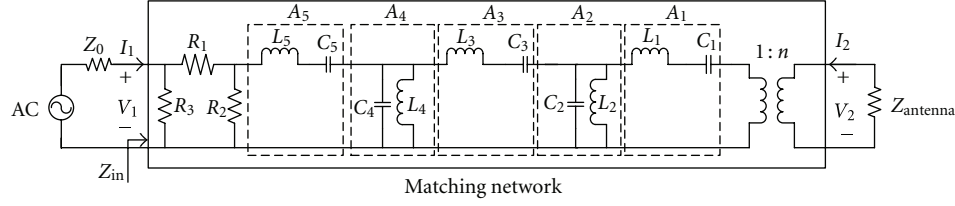


FIGURE 1: Topology of the matching network.

and an impedance transformer. The series component of the T-network is the LC series resonant circuit and the parallel component is the LC parallel resonant circuit. The elements of the resistor network are resistors; although the resistors will reduce the efficiency of the network, they and the transformer together can match the T-network to the antenna better.

The matching network was used for the wideband VHF/UHF antenna proposed in [14]. The VHF/UHF antenna without matching networks has a VSWR of less than 2.5 from 200 to 447 MHz. The overall height of the antenna is only  $0.087\lambda_{\max}$ , where  $\lambda_{\max}$  is the largest wavelength that corresponds to the lowest frequency of 200 MHz. It has met the requirements of applications required by our industrial sponsors except the height and diameter. The required height and diameter of the antenna are reduced further to  $0.069\lambda$  and  $0.375\lambda$ , respectively, where  $\lambda$  is the wavelength of 225 MHz. In recognizing the difficulty in achieving standard low VSWR with such an electrically small antenna over a frequency band of 225 to 400 MHz, the requirement for VSWR is relaxed to  $\text{VSWR} < 3$ . Such a relaxation of the VSWR requirement happens in some applications; for example, in [15–18], the VSWR was specified in the range of 3.0 to 6.0.

To achieve  $\text{VSWR} < 3$  with the reduced size, the impedance matching network is added, analyzed, and then optimized with the proposed algorithm as described hereinafter.

First, the transfer function of the overall matching network is found by cascading the transfer functions of every series or parallel elements. For the T impedance network, they can be written, respectively, as (see Figure 1) follows:

$$\mathbf{A}_1 = \begin{bmatrix} 1 & j\omega L_1 + \frac{1}{j\omega C_1} \\ 0 & 1 \end{bmatrix},$$

$$\mathbf{A}_2 = \begin{bmatrix} 1 & 0 \\ j\omega C_2 + \frac{1}{j\omega L_2} & 1 \end{bmatrix},$$

$$\mathbf{A}_3 = \begin{bmatrix} 1 & j\omega L_3 + \frac{1}{j\omega C_3} \\ 0 & 1 \end{bmatrix},$$

$$\mathbf{A}_4 = \begin{bmatrix} 1 & 0 \\ j\omega C_4 + \frac{1}{j\omega L_4} & 1 \end{bmatrix},$$

$$\mathbf{A}_5 = \begin{bmatrix} 1 & j\omega L_5 + \frac{1}{j\omega C_5} \\ 0 & 1 \end{bmatrix}.$$

(1)

For the resistor network, the transfer functions of every element are

$$\mathbf{A}_{R_1} = \begin{bmatrix} 1 & R_1 \\ 0 & 1 \end{bmatrix}, \quad \mathbf{A}_{R_2} = \begin{bmatrix} 1 & 0 \\ \frac{1}{R_2} & 1 \end{bmatrix},$$

(2)

$$\mathbf{A}_{R_3} = \begin{bmatrix} 1 & 0 \\ \frac{1}{R_3} & 1 \end{bmatrix}.$$

For the transformer, the transfer function is

$$\mathbf{A}_n = \begin{bmatrix} \frac{1}{n} & 0 \\ 0 & n \end{bmatrix}.$$

(3)

Then, the transfer function of the overall matching network is then

$$\mathbf{A}_{\text{network}} = \mathbf{A}_{R_3} \mathbf{A}_{R_1} \mathbf{A}_{R_2} \mathbf{A}_5 \mathbf{A}_4 \mathbf{A}_3 \mathbf{A}_2 \mathbf{A}_1 \mathbf{A}_n = \begin{bmatrix} a & b \\ c & d \end{bmatrix},$$

(4)

where  $a$ ,  $b$ ,  $c$ , and  $d$  are the elements of the transfer matrix that can be found through (4).

The input impedance  $Z_{\text{in}}(\omega)$  of the matching network, as seen in Figure 1, can be expressed as

$$Z_{\text{in}} = \frac{\dot{V}_1}{\dot{I}_1} = \frac{a\dot{V}_2 + b(-\dot{I}_2)}{c\dot{V}_2 + d(-\dot{I}_2)} = \frac{aZ_{\text{antenna}} + b}{cZ_{\text{antenna}} + d},$$

(5)

where  $Z_{\text{antenna}}$  is the impedance of the antenna.

The reflection coefficient is a function of the input impedance:

$$\Gamma(\omega) = \frac{Z_{\text{in}}(\omega) - Z_0}{Z_{\text{in}}(\omega) + Z_0},$$

(6)

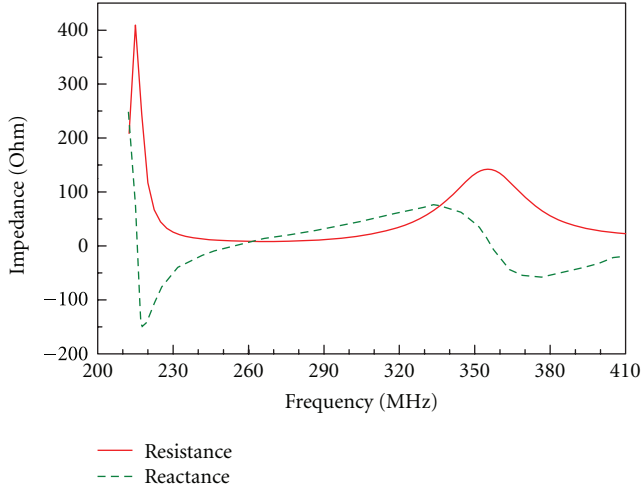


FIGURE 2: Impedance of the wideband VHF/UHF antenna with the reduced height of  $0.069\lambda$  and diameter of  $0.375\lambda$ .

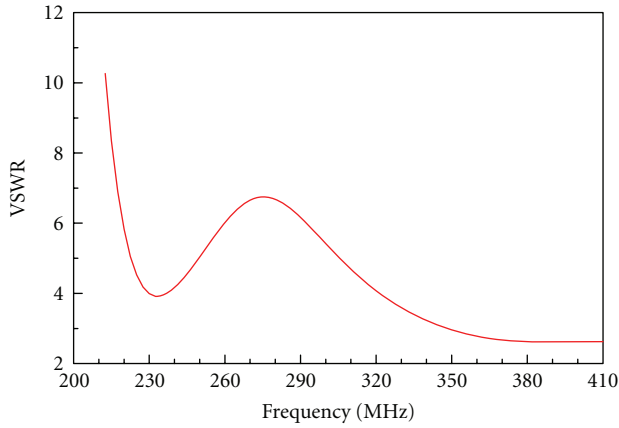


FIGURE 3: VSWR of the wideband VHF/UHF antenna with the reduced height of  $0.069\lambda$  and diameter of  $0.375\lambda$ .

where  $Z_0$  is the characteristic impedance of the feeding line, and it is assumed to be 50 Ohm.

With (5) and (6), two important antenna parameters are found: one is VSWR which is

$$\text{VSWR}(\omega) = \frac{1 + |\Gamma(\omega)|}{1 - |\Gamma(\omega)|}, \quad (7)$$

another is transducer power gain (TPG), which is defined as the ratio of the maximum power available from the source to the power delivered to the antenna [9]; it can be found as

$$\text{TPG}(\omega) = \frac{4|z_{21}|^2 Z_0 \text{Re}(Z_{\text{antenna}})}{|(z_{11} + Z_{\text{in}})(z_{22} + Z_{\text{antenna}}) - z_{12}z_{21}|^2}. \quad (8)$$

Here  $z_{11}$ ,  $z_{12}$ ,  $z_{21}$ , and  $z_{22}$  are the elements of the impedance matrix of the overall matching network; they can be obtained by converting the transfer matrix of (4) as described in [19].

As mentioned before, the antenna under consideration is the wideband low-profile disccone-based antenna proposed in [14] but with a reduced size; it has a height of  $0.069\lambda$  and

a diameter of  $0.375\lambda$ , where  $\lambda$  is the wavelength of 225 MHz. The antenna impedance  $Z_{\text{antenna}}$  without the matching network is shown in Figure 2. The corresponding VSWR of the antenna is shown in Figure 3. In Section 3, the matching is added as shown in Figure 1 and the GA-SA is applied to optimize the matching network to reduce the VSWR.

### 3. The GA-SA Algorithm and Its Application to Optimize the Matching Network

GA and SA are two of the most popular optimization techniques. GA is a robust optimization tool based on biology evolution theory [9]. It simulates gene recombine and evolution process, including natural selection, crossover, and mutation operators. With iterative operations, the best solution can be obtained for a system.

In general, the rate of convergence of a global optimization technique depends on proper choice of design parameters and rules of evolution. GA has the advantages of that it does not require derivative information, and it is well suited for parallel searches from a wide sampling. However, the GA process can be slow, especially when it closes in the neighborhood of the best solution [9].

SA originated from emulation of the process of solid material annealing in the material science field [11] and is now widely utilized in numerical parameter optimization. In the annealing process, a substance is heated above its melting temperature and then gradually cooled down to minimize its energy distribution. SA emulates such a process and is generally more reliable in finding the global optimum. It does not require derivative computation and is a zero-order algorithm like GA. However, SA is highly dependent on the initial temperatures or initial parameters; it may not be as robust as GA if initial parameters are not well chosen [13]. More discussion and implementation issues of GA and SA can be found in [20, 21].

From the previous observations above, we conclude that GA and SA have complementary advantages and disadvantages. Therefore, a hybrid GA-SA algorithm should combine the advantages of the two methods while circumvent the disadvantages. GA is not sensitive to initial starting parameters. It can iterate fast to nearby the optimal solution; then SA takes over. Due to the good initial parameters from GA, only a small number of iterations are needed for SA to obtain the optimal solution.

In other words, GA and SA are combined in such a way that GA is applied for the first part of the optimization process, while SA is employed for the second part. GA starts the initial phase of the optimization and provides its values as the initial parameters of SA which forms the second phase of the optimization; as a result, fast convergence to an optimized solution is expected.

In the following subsections, implementation details of the combined SA-GA optimization are described.

**3.1. Chromosome Specification in GA.** The proposed matching network consists of resistors, reactive elements, and an ideal transformer. Altogether there are 14 elements in

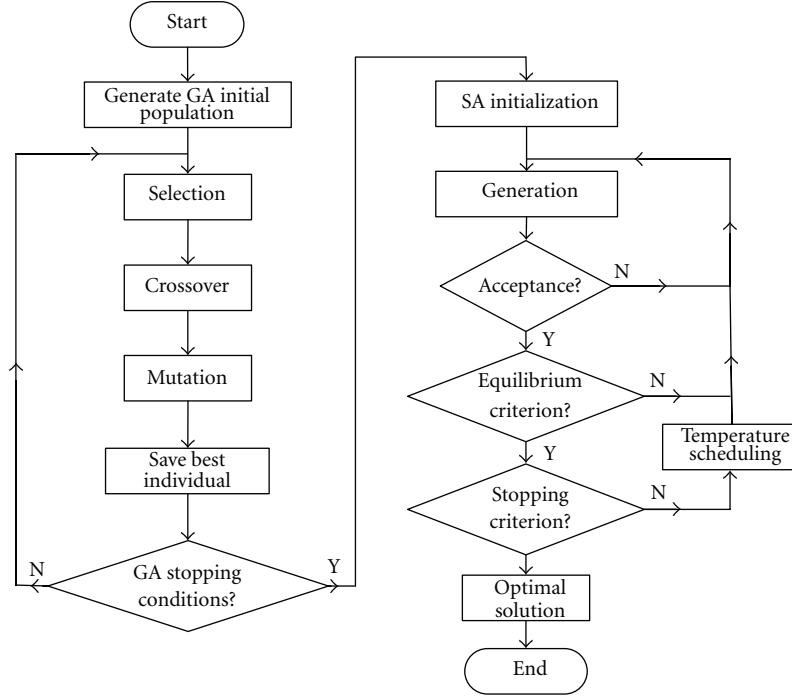


FIGURE 4: Flowchart of GA-SA.

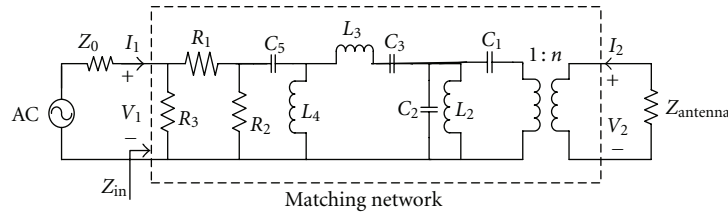


FIGURE 5: Optimized matching network.

TABLE 1: Control parameters of GA-SA.

GA parameters	Values	SA parameters	Values
Number of individuals	200	Initial temperature	0.05
Initial crossover probability	0.9	Terminated temperature	0.00001
Initial mutation probability	0.015	Annealing rate	0.9
Generation gap	0.9	—	—
Number of generations	250	—	—

TABLE 2: Optimal values of matching network elements.

Elements	Values	Elements	Values
$n$	0.88	$R_1$	7.2 $\Omega$
$R_2$	955 $\Omega$	$R_3$	900 $\Omega$
$L_1$	1.8 pF	$C_1$	23 pF
$L_2$	18 nH	$C_2$	9 pF
$L_3$	10 nH	$C_3$	7.8 pF
$L_4$	25 nH	$C_4$	0 pF
$L_5$	1.1 pF	$C_5$	15 pF

the network. A real-coded GA is used in this paper: behaviors of each element are described by a real vector of the elements:

$$\mathbf{X} = [n, R_1, R_2, R_3, L_1, C_1, L_2, C_2, L_3, C_3, L_4, C_4, L_5, C_5], \quad (9)$$

where  $n$  is the turn ratio of the ideal transformer;  $R_i$  ( $i = 1, 2, 3$ ),  $L_i$  ( $i = 1, 2, 3, 4, 5$ ), and  $C_i$  ( $i = 1, 2, 3, 4, 5$ ) are the values of the resistors, inductors, and capacitors in the

matching network, respectively. The GA-SA algorithm will then give the optimized real vector after the optimization.

The admissible value ranges of each element are  $0.1 \leq n \leq 10$ ,  $0 < R_i \leq 5 \text{ k}\Omega$ ,  $0 < L_i \leq 1.0 \mu\text{H}$ , and  $0 < C_i \leq 800 \text{ pF}$ , based on the practical considerations provided by the industrial sponsor of this work.

**3.2. Objective Functions.** The optimization is carried out in respect to VSWR and TPG over a wide frequency band.

TABLE 3: Comparisons of the results with different algorithms.

Algorithm	Number of individuals in GA	Generations in GA	Initial parameters in SA	Initial temperature in SA	Terminated temperature in SA	Matching network performance	
						VSWR	TPG
GA	200	400				<4	>45%
SA			Random	0.05	0.000001	<4	>36%
GA-SA	200	250	Optimal parameters in GA	0.05	0.00001	<3	>59%

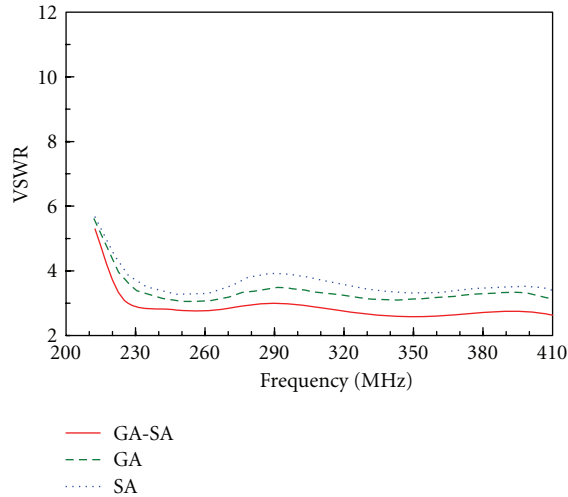


FIGURE 6: VSWR obtained with different techniques.

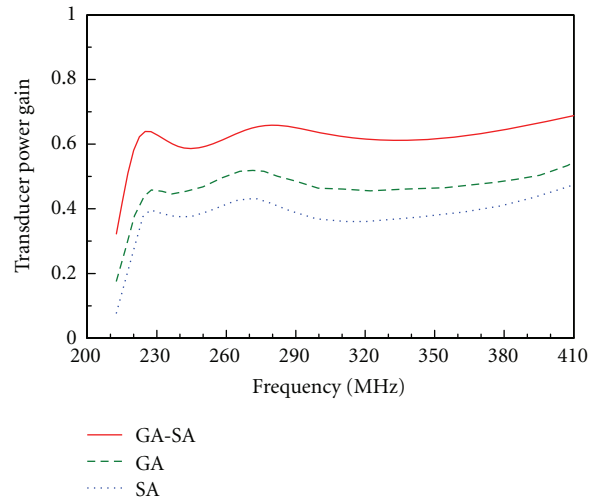


FIGURE 7: TPG of the matching network.

Therefore, the design is a multiobjective optimization problem. The objective function is then defined as

$$f = \begin{cases} \min \left\{ \sum_{i=1}^N \text{VSWR}(\omega_i) \right\}, \\ \max \left\{ \sum_{i=1}^N \text{TPG}(\omega_i) \right\}, \end{cases} \quad (10)$$

where  $N$  is the total number of frequency points selected for optimization in the frequency band of interest.

**3.3. Combination of GA and SA.** As indicated before, the proposed optimization process starts with the GA process and then SA process. The stopping condition for the GA process is either that a given number of generations of GA are reached (which is taken to be 250 in this paper), or that negligible further improvement of the objective functions is observed.

The complete optimization flowchart is shown in Figure 4.

## 4. Optimization Results

The GA-SA algorithm is applied and the control parameters of the algorithm are listed in Table 1.

With the GA-SA optimization, the optimal values of the matching network elements are obtained as presented in Table 2.

As shown in Table 2, the values of  $L_1$ ,  $L_5$ , and  $C_4$  are so small that these three elements present no utility and are therefore eliminated from the network. The final optimized matching network is depicted in Figure 5.

The VSWR of the antenna, after the optimization by GA-SA, is shown in Figure 6. We can see that VSWR is much improved after addition of the optimized matching network and the bandwidth of  $\text{VSWR} < 3$  now covers a frequency range from 225 MHz to 400 MHz, which meets the requirement set by the industrial sponsor of this work.

For comparison, two VSWR results, after the optimization with GA and SA, respectively, are also shown in Figure 6. Both of them are less than 4 in the operating frequency band but larger than that obtained with the proposed combined GA and SA algorithm.

Figure 7 is the TPG of the matching network. With the matching network optimized with GA-SA, the TPG is greater than 59% within the whole bandwidth. With GA and SA, it is only 45% and 36%, respectively.

The comparison of GA-SA, GA, and SA in terms of convergence is given in Figure 8. In Figure 8, the errors are computed in reference to the optimization targets for the algorithms over the whole bandwidth. The optimization results with GA-SA, GA, and SA are shown in Table 3. It can be seen that the optimized results with GA-SA are better than those with GA or SA alone. In addition the combined GA-SA method used fewer numbers of generations or iterations.

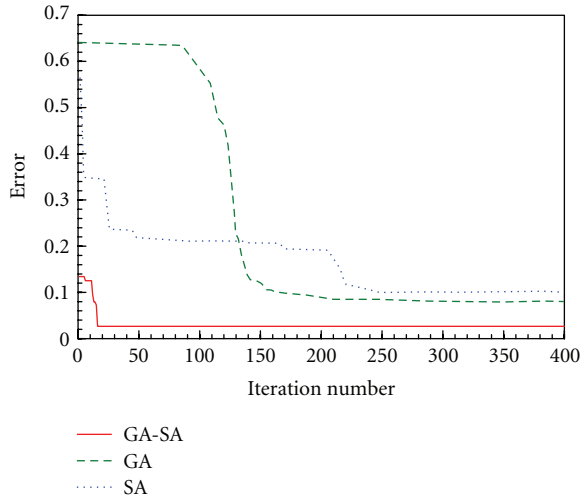


FIGURE 8: Comparison of GA-SA, GA, and SA in terms of convergence.

In other words, the performances of the combined GA-SA method exceed over those of the GA and SA alone.

## 5. Conclusion

In this paper, an algorithm combining GA and SA is developed and applied to optimization of a wideband matching network for antennas. By adding the matching network for a discone-based VHF/UHF antenna and then optimizing it, the proposed algorithm is demonstrated to be efficient and effective since it takes advantages of both GA and SA. In other words, the GA-SA-combined method is an effective technique for optimization.

## Acknowledgments

This work was supported in part by the National Science Foundation of China and NSAF under their joint Grant (no. 11076031).

## References

- [1] B. K. Lau, J. B. Andersen, G. K. Senior et al., "Impact of matching network on bandwidth of compact antenna arrays," *IEEE Transactions on Antennas and Propagation*, vol. 54, no. 11, pp. 3225–3238, 2006.
- [2] J. T. Aberle, "Two-port representation of an antenna with application to non-foster matching networks," *IEEE Transactions on Antennas and Propagation*, vol. 56, no. 5, pp. 1218–1222, 2008.
- [3] A. Van Bezooijen, M. A. De Jongh, F. Van Straten, R. Mahmoudi, and A. H. M. Van Roermund, "Adaptive impedance-matching techniques for controlling 1 networks," *IEEE Transactions on Circuits and Systems I*, vol. 57, no. 2, pp. 495–505, 2010.
- [4] F. Paredes, G. Z. Gonzalez, J. Bonache, and F. Martín, "Dual-band impedance-matching networks based on splitting resonators for applications in rf identification (RFID)," *IEEE Transactions on Microwave Theory and Techniques*, vol. 58, no. 5, pp. 1159–1166, 2010.
- [5] M. Selvanayagam and G. V. Eleftheriades, "A compact printed antenna with an embedded double-tuned metamaterial matching network," *IEEE Transactions on Antennas and Propagation*, vol. 58, no. 7, pp. 2354–2361, 2010.
- [6] O. M. Ramahi and R. Mittra, "Design of a matching network for an hf antenna using the real frequency method," *IEEE Transactions on Antennas and Propagation*, vol. 37, no. 4, pp. 506–509, 1992.
- [7] A. Chen, Y. Zhang, T. Jiang, and D. Su, "Optimal design of broadband matching network for electrically small antennas," *Journal of Beijing University of Aeronautics and Astronautics*, vol. 35, no. 11, pp. 1311–1319, 2009.
- [8] K. Yegin and A. Q. Martin, "On the design of broad-band loaded wire antennas using the simplified real frequency technique and a genetic algorithm," *IEEE Transactions on Antennas and Propagation*, vol. 51, no. 2, pp. 220–228, 2003.
- [9] J. L. Rodríguez, I. García-Tuñón, J. M. Taboada, and F. Obelleiro Basteiro, "Broadband hf antenna matching network design using a real-coded genetic algorithm," *IEEE Transactions on Antennas and Propagation*, vol. 55, no. 3, pp. 611–618, 2007.
- [10] X. Ding, B. Z. Wang, G. Zheng, and X. M. Li, "Design and realization of a ga-optimized vhf/uhf antenna with "on-body" matching network," *IEEE Antennas and Wireless Propagation Letters*, vol. 9, pp. 303–306, 2010.
- [11] J. Martínez-Fernández, J. M. Gil, and J. Zapata, "Ultrawideband optimized profile monopole antenna by means of simulated annealing algorithm and the finite element method," *IEEE Transactions on Antennas and Propagation*, vol. 55, no. 6, pp. 1826–1832, 2007.
- [12] Y. Zhang and W. Q. Malik, "Analogue filter tuning for antenna matching with multiple objective particle swarm optimization," in *IEEE/Sarnoff Symposium on Advances in Wired and Wireless Communication*, pp. 196–198, April 2005.
- [13] S. Xavier-De-Souza, J. A. K. Suykens, J. Vandewalle, and D. Bolle, "Coupled simulated annealing," *IEEE Transactions on Systems, Man, and Cybernetics B*, vol. 40, no. 2, pp. 320–335, 2010.
- [14] A. Chen, T. Jiang, Z. Chen, D. Su, W. Wei, and Y. Zhang, "A wideband vhf/uhf discone-based antenna," *IEEE Antennas and Wireless Propagation Letters*, vol. 10, pp. 450–453, 2011.
- [15] M. E. Bialkowski, A. R. Razali, and A. Boldaji, "Design of an ultrawideband monopole antenna for portable radio transceiver," *IEEE Antennas and Wireless Propagation Letters*, vol. 9, pp. 554–557, 2010.
- [16] K. J. Kim, S. Lee, B. N. Kim, J. H. Jung, and Y. J. Yoon, "Small antenna with a coupling feed and parasitic elements for multi-band mobile applications," *IEEE Antennas and Wireless Propagation Letters*, vol. 10, pp. 290–293, 2011.
- [17] S. D. Rogers and C. M. Butler, "Wide-band sleeve-cage and sleeve-helical antennas," *IEEE Transactions on Antennas and Propagation*, vol. 50, no. 10, pp. 1409–1414, 2002.
- [18] D. H. Choi, H. S. Yun, and S. O. Park, "Internal antenna with modified monopole type for DVB-H applications," *Electronics Letters*, vol. 42, no. 25, pp. 1436–1438, 2006.
- [19] D. M. Pozar, *Microwave Engineering*, John Wiley & Sons, New York, NY, USA, 2nd edition, 1998.
- [20] R. L. Haupt and S. E. Haupt, *Practical Genetic Algorithms*, John Wiley & Sons, New York, NY, USA, 2nd edition, 2004.
- [21] C. M. Tan, *Simulated Annealing*, In-Teh, 2008.



**Hindawi**

Submit your manuscripts at  
<http://www.hindawi.com>

